Astron. Astrophys. 355, 347–354 (2000)

ASTRONOMY AND ASTROPHYSICS

Multi-mode oscillations of sunspots

Y.D. Zhugzhda[1,2], **H. Balthasar**[1], **and J. Staude**[1]

[1] Astrophysikalisches Institut Potsdam, Sonnenobservatorium Einsteinturm, 14473 Potsdam, Germany (yzhugzhda@aip.de; hbalthasar@aip.de; jstaude@aip.de)

[2] Institute of Terrestrial Magnetism, Ionosphere and Radio Wave Propagation of the Russian Academy of Sciences, Troitsk city, Moscow Region, 142092 Russia (yuzef@izmiran.rssi.ru)

Received 25 June 1999 / Accepted 10 December 1999

Abstract. Oscillations of the magnetic field in the sunspot photosphere have been detected by recent high-resolution, two-dimensional observations. Their power is concentrated in isolated small flux bundles (pores) outside of larger umbrae and at the boundary between umbra and penumbra of larger spots. The slow body mode provides an explanation of the appearance of magnetic oscillations in small sunspots if the azimuth number $m = 0$, but also of the small features piling up in rings in large sunspots. In the latter model the magnetic oscillations are the signature of the slow body mode with $m \gg 1$, which bears a resemblance to the well-known whispering gallery mode in acoustics. The slow surface modes and fast body modes are also discussed.

Key words: Sun: atmosphere – Sun: magnetic fields – Sun: oscillations – Sun: sunspots

1. Introduction

Sunspots show oscillations of velocity v (Doppler shifts), of intensity I (that is, of thermodynamic quantities), and of geometrical displacements of the line or continuum forming layers, if the sunspot is observed close to the limb. The analyses of the time series often display sharp power peaks which are closely packed and concentrated in period bands around 2...3 min, 5 min, and $\gtrsim 20$ min, the oscillations of which are likely produced by different physical mechanisms. Observations of such eigen-oscillations of sunspots are known for more than 25 years; recent reviews are given, e.g., by Lites (1992) and by Staude (1999).

The results of earlier attempts to measure oscillations of the magnetic field at photospheric levels of sunspots were contradictory (Staude 1999). There were only a few papers reporting oscillatory power of magnetic field components in the 3-min and 5-min period bands. Latest one-dimensional data obtained by Lites et al. (1998) with the Advanced Stokes Polarimeter found an upper limit of 4 G (rms) of the magnetic field oscillations; the authors included a model of eigen-modes due to magneto-atmospheric waves in a homogeneous, vertical magnetic field.

Send offprint requests to: J. Staude

The situation changed when two-dimensional data of high quality became available: Observations with a Fabry-Perot interferometer (FPI) at the Vacuum Tower Telescope (VTT) on Tenerife (Horn et al. 1997; Balthasar 1998, 1999) and with the Michelson Doppler Imager (MDI) onboard SOHO (Rüedi et al. 1998; Rüedi & Solanki 1999; Norton et al. 1998, 1999) have shown that significant magnetic field oscillations exist, but they are limited to much smaller regions inside the spots than the well known velocity oscillations which cover large parts of a sunspot.

In order to explain these data, new approaches and ideas are required. So far, the modelling of sunspot oscillations has considered a 'global' mode only, where the whole sunspot is involved in the oscillations with the same frequency. This approach proved to be very successful in explaining the basic features of the observed spectrum of oscillatory power peaks in the 3-min and 5-min period bands mentioned above (Uchida & Sakurai 1975; Scheuer & Thomas 1981; Thomas & Scheuer 1982; Žugžda et al. 1983, 1984, 1987; Gurman & Leibacher 1984; Wood 1997; Gore 1998).

However, the new data show a strong spatial intermittance of oscillations, with frequencies varying across the sunspot. Thus, it is reasonable to assume that different wave modes coexist in a sunspot. Another unresolved problem of the theory is the appearance of significant power of magnetic oscillations, which should be negligible in the case of the 'global' mode (see Lites et al. 1998).

In the current paper we will shortly describe some details of our recent FPI-VTT observations. Then we propose an explanation of the appearance of magnetic oscillations on small scales, which is based on the general properties of the slow mode in magnetic flux tubes. A new mode is taken into consideration which is related to the concentration of magnetic oscillations in rather thin features concentrated along the umbra-penumbra boundary.

2. Observations

In our observations the VTT at Tenerife has been used, partly together with a polarimeter in front of a two-dimensional imaging spectrometer with an FPI. The spectrometer has been described by Bendlin et al. (1992), the remaining instrumentation, calibration, and data reduction by Horn et al. (1996). Narrow-band filtergrams are recorded on a CCD camera with 0.”2 pixels. Image blurring usually results in a real spatial resolution of better than 0.”8 for the best images and 1.”0 on the average during good seeing conditions.

A first time series (case 1) was obtained on July 20, 1994, and was focused on the main spot of the active region NOAA 7757, 30° NE from the disk center; details are described by Horn et al. (1997). This has been the first report of magnetic oscillations discovered in two-dimensional, high-resolution sunspot observations; the results initiated a controversial discussion.

A second data set of 114 min length (case 2) was taken from the preceding spot of NOAA 8076 on August 28, 1997 ($30°$ N, $35°$ E) applying the same instrumentation as above, but without the polarimeter (a larger field of view of $57” \times 48”$ is obtained in this way), and using the line Fe I 6843 Å (Balthasar 1998, 1999). The spectral spacing was 12.9 mÅ. The magnetic splitting is determined by fitting theoretical Stokes I profiles to the observed profiles, resulting in a quantity which is close to the absolute value B of the magnetic field vector $\boldsymbol{B}$. In case 1, using the circularly polarized spectra, we derive a quantity which is closer to the line-of-sight component B_l of $\boldsymbol{B}$ if the Zeeman splitting is not complete.

The main results can be summarized as follows: the strongest power of magnetic field oscillations was concentrated in the centres of small spots or pores, which were found outside the large spots. In the larger spots enhanced magnetic power is found mainly at the boundary between umbra and penumbra, that is in a ring-like structure, while velocity power covers a great part of the umbra (see Balthasar 1999). Enhanced magnetic (and velocity) power is also found in dark patches inside the penumbra (see Fig. 1). The ring-like structure has fine substructures with diameters of $\lesssim 1.”5$. These structures are visible for a broader range of periods. In case 2 no clear correlation between the fluctuations of B and v or I could be found. In case 1, however, there is a strong coherence between the oscillations of B_l and v, mainly in a horseshoe-like structure at the centre-side boundary between umbra and penumbra and strongest in the 3-min band. Both types of oscillations are in phase here, while there is rather a phase difference of π in the penumbra for the 5-min oscillations. In case 2 we find a ratio BV of the oscillation amplitudes of magnetic field and velocity (see Eqs. (10) and (11)) of about 2.2 for the 5-min and 1.4 for the 3-min periods. However, it has to be kept in mind that these ratios cannot be determined very accurately from the present data, and the uncertainty of the derived phase relations is still large.

3. Modelling: Wave modes in magnetic fluxtubes

So far theoretical models of sunspot oscillation have treated the sunspot as an axi-symmetric, vertical tube with a constant magnetic field. Main emphasis was given on the stratification and on the upper and lower boundary conditions, while the effect of the surrounding atmosphere on the oscillations was largely ignored. In order to explore that effect we consider here a model of an intense flux tube with a uniform, vertical magnetic field

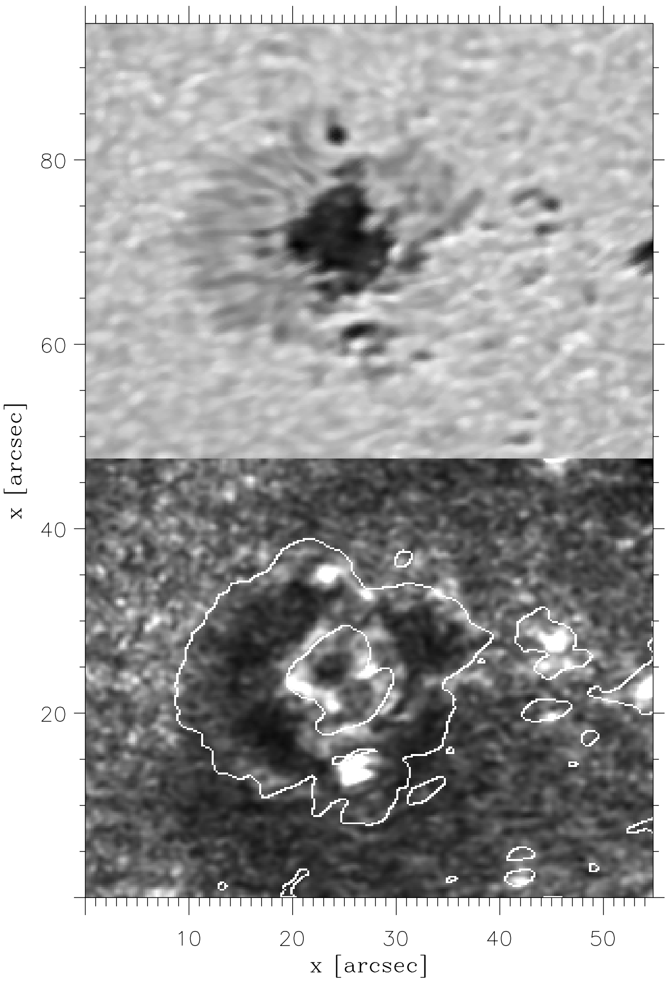

Fig. 1. Top: Single white-light image of the leading sunspot of NOAA 8076 (case 2). Bottom: Power map of oscillations of the magnetic field strength in the 3 min period range (4.9 – 6.4 mHz) for the same sunspot. White indicates high power. In order to enhance the contrast of small features, power values above 1000 $G^2\,mHz^{-1}$ are truncated. The white lines indicate the outer boundaries of the magnetic features in the averaged continuum intensity image as well as the boundary between umbra and penumbra.

embedded in a plasma with a weaker B_e outside ($B_e = 0$ will be assumed in the further discussion). We ignore the effect of stratification, but we take into account the effect of the surroundings. The temperature T of the plasma outside the tube is higher than inside: The effective T differ by 2000 K, but due to the Wilson effect the real difference of T at equal geometrical heights z is much higher – at $T = 3600$ K, a typical value in the umbral line-forming layer, we have $T \gtrsim 12000$ K outside in the surrounding convective zone.

The theory of linear waves in flux tubes is well developped (see, for example, Roberts 1992). This allows to consider all wave modes in our simple model. As a first step we describe a new method for treating the dispersion relation originally derived by Edwin & Roberts (1983).

3.1. The dispersion relation

The dispersion relation for axi-symmetric body waves in an intense flux tube, taking into account the effect of the surroundings, was derived by Edwin & Roberts (1983):

$$\rho_0(k^2C_A^2-\omega^2)m_e\frac{K_{m+1}(m_eR)}{K_m(m_eR)}-$$
$$-\rho_{0e}(k^2C_{Ae}^2-\omega^2)n_o\frac{J_{m+1}(n_0R)}{J_m(n_0R)}\;=\;0, \qquad (1)$$

where n_0 and m_e are

$$n_0^2=-\frac{(k^2C_S^2-\omega^2)(k^2C_A^2-\omega^2)}{(C_S^2+C_A^2)(k^2C_T^2-\omega^2)}>0,$$

and

$$m_e^2=\frac{(k^2C_{Se}^2-\omega^2)(k^2C_{Ae}^2-\omega^2)}{(C_{Se}^2+C_{Ae}^2)(k^2C_{Te}^2-\omega^2)}>0.$$

J_m and K_m are Bessel functions of order $m. C_S, C_{Se}, C_A, C_{Ae}, C_T, C_{Te},\ \rho_0, \rho_{0e}$ are the sound, Alfvén and tube speeds and mass density inside and outside the tube, respectively, and R is the tube radius. We restrict our consideration to the special case, when the external magnetic field is absent.

Let us introduce the dimensionless parameters

$$\beta=\frac{C_S^2}{C_A^2},\quad \delta=\frac{C_{Se}^2}{C_S^2},\ \Delta=\frac{\rho_{0e}}{\rho_0}=\frac{2\beta+\gamma}{2\delta\beta}, \qquad (2)$$

and the dimensionless variables

$$x=kR,\quad \Omega=\frac{\omega}{kC_T},\quad j^2=n_0^2R^2. \qquad (3)$$

The dispersion relation in the dimensionless variables reads

$$(1+\beta-\beta\Omega_b^2)m_bx\frac{K_{m+1}(m_bx)}{K_m(m_bx)}+\beta\Omega_b^2\Delta j\frac{J_{m+1}(j)}{J_m(j)}=0, \qquad (4)$$

where

$$m_b=\sqrt{\frac{\delta(1+\beta)-\Omega_b^2}{\delta(1+\beta)}},\quad \Omega_b^2=\frac{2}{1\pm\sqrt{1-4\beta x^2a^{-1}}}, \qquad (5)$$

and

$$a=(1+\beta)^2(x^2+j^2).$$

This is the dispersion relation for slow and fast body waves. The choice of the plus sign in (5) corresponds to slow waves, while fast waves correspond to the choice of minus. The slow surface waves are described by a similar dispersion relation, where the Bessel functions J have to be replaced by the modified Bessel functions I, j^2 has to be replaced by $-j^2$, $m=0$, and the choice of the sign in (5) is plus.

The derived version of the dispersion relation has the advantage that separate dispersion relations for different wave modes can be derived. A numerical treatment of the dispersion relation is simplified considerably in this case, because it is reduced to the solution of Eq. (4) with respect to j for given values of x, β, Δ, and δ. After calculating j, the frequency can be found by substituting j in (5). We would like to remind that the dispersion relation takes into account a reaction of the surrounding plasma, because it is the result of matching the solutions inside and outside the tube.

3.2. Amplitudes and phases of velocity and magnetic oscillations

For linear running waves in a vertical magnetic tube, the relative values of oscillations of velocity and of the magnetic field as a function of radius r and azimuth angle ϕ (similar expressions for $m=0$ are given by Roberts & Webb 1978) are

$$\frac{V_z}{C_S}\;=\;-\frac{iA_0k_zC_S}{\omega^2}J_m\left(\frac{jr}{R}\right)e^{im\phi+i\omega t+ik_zz}, \qquad (6)$$
$$\frac{\delta B_z}{B_z}\;=\;\frac{iA_0(\omega^2-k_z^2C_S^2)}{\omega^3}J_m\left(\frac{jr}{R}\right)e^{im\phi+i\omega t+ik_zz}, \qquad (7)$$
$$\frac{V_r}{C_S}\;=\;\frac{A_0(\omega^2-k_z^2C_S^2)R}{j\omega^2C_S}J_{m+1}\left(\frac{jr}{R}\right)e^{im\phi+i\omega t+ik_zz}, \qquad (8)$$
$$\frac{\delta B_r}{B_z}\;=\;\frac{A_0(\omega^2-k_z^2C_S^2)k_zR}{j\omega^3}J_{m+1}\left(\frac{jr}{R}\right)e^{im\phi+i\omega t+ik_zz}, \qquad (9)$$

where A_0 is an arbitrary constant and j is a root of the dispersion relation. In the case of standing waves the exponents in (6 - 9) have to be replaced by $\cos\omega t\sin k_zz$ for V_z and δB_r and by $\sin\omega t\cos k_zz$ for δB_z and V_r.

The ratio of the relative amplitudes of the magnetic field and the longitudinal velocity oscillations for body waves follows from Eqs. (6-7):

$$BV=\frac{\delta B_z}{B_z}\Big/\frac{V_z}{C_S}=\frac{k_z^2C_S^2-\omega^2}{\omega k_zC_S}=\frac{1+\beta-\Omega_b^2}{\Omega_b\sqrt{1+\beta}}. \qquad (10)$$

This expression provides a simple way to compare different wave modes from the point of view of the relative size of velocity and magnetic field amplitudes. It is important to point out that the ratio of amplitudes BV (10) is valid for the case of running waves. In the case of standing waves the ratio of amplitudes depends on the position of the observing point with respect to positions of nodes of the standing wave

$$BV=\frac{\delta B_z}{B_z}\Big/\frac{V_z}{C_S}=\frac{1+\beta-\Omega_b^2}{\Omega_b\sqrt{1+\beta}}\cot k_zz. \qquad (11)$$

So, if we are close to a node of the vertical velocity, BV for standing waves exceeds the value for running waves. In the case of a slow body wave the phase velocity tends to the tube speed $\omega/k_z\to C_T$ ($\Omega_b\to 1$) in the limit of a thin tube ($x=k_zR\to 0$). This follows from Eq. (5), because, for example, in the case of $m=0$ the root of the dispersion relation falls in the range $2.4<j<3.8$ for any values of x. Consequently, in the limit of a thin flux tube the ratio of magnetic and velocity amplitudes for slow body waves is

$$BV=\frac{\beta}{\sqrt{1+\beta}}. \qquad (12)$$

The opposite limit of a very thick tube corresponds to a longitudinal ($k_\perp=0$) propagation of slow waves in a uniform magnetic field. In this case the phase velocity equals the sound speed C_S, because the uniform magnetic field does not affect the longitudinal motions of the plasma. Consequently, in this limit $BV=0$, because magnetic oscillations do not arise. This correspond to observations, which show magnetic oscillations

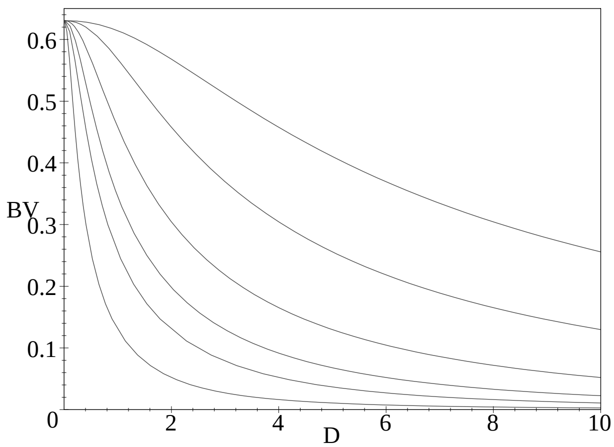

Fig. 2. The dependence of BV in Eq. (10), the ratio of the relative amplitudes of magnetic and velocity oscillations, on the sunspot diameter D (in 10^3 km) for periods of 20 min (top curve), 10, 5, 3, 2, and 1 min (bottom curve).

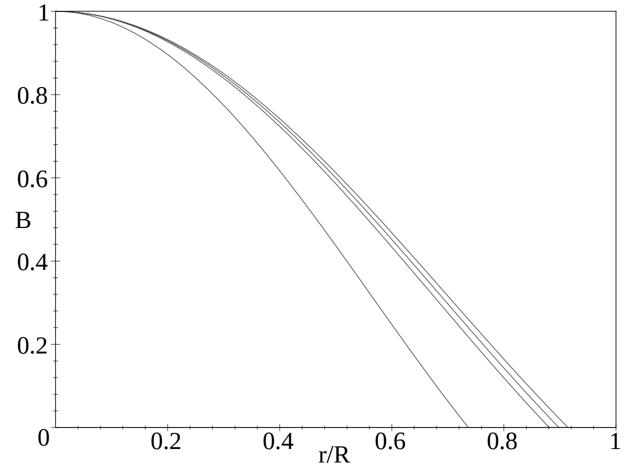

Fig. 3. The dependence of the amplitude of longitudinal magnetic field oscillations B_z, normalized to its maximum value, on the radius r for slow body waves in units of the sunspot radius of R, for $R = 5 \cdot 10^3$ (right curve), $2 \cdot 10^3$, $1 \cdot 10^3$, and $1 \cdot 10^2$ km (left curve); the period is 300 s.

in small sunspots and no global magnetic oscillations in large sunspots.

In the case of fast body waves, the phase velocity tends to $\sqrt{C_A^2 + C_S^2}$ in the limit of a thin flux tube and to the C_A in the limit of a thick flux tube. Thus, the ratio of amplitudes (10) for a thick tube is

$$BV = \frac{\beta - 1}{\sqrt{1+\beta}}, \tag{13}$$

and the ratio $BV = 0$ for the thin flux tube. Thus, the properties of fast body waves do not fit the results of observations. Moreover, the fast mode in a tube is transverse, which neither fits the observations.

The phase speed of slow surface mode does not depend strongly on the tube size, it is close to the tube speed C_T. Thus, the ratio of magnetic and velocity amplitudes is approximately given by (12). The power of the oscillations of the surface mode is concentrated along the border of the tube. Thus, it is a candidate for an explanation of magnetic oscillations along the border in large sunspots.

3.3. The slow body 'global' mode

The described analysis gave hints at wave modes which could be good candidates for an explanation of the sunspot oscillations. First, we consider 'global' oscillations, when the whole sunspot oscillates in phase, corresponding to the case $m = 0$. The slow body mode could provide an explanation, but it is not clear from the above analysis which sizes of sunspots correspond to the limits of thin and thick flux tubes. To clarify the question, numerical calculations of the ratio BV for the slow body mode with $m = 0$ were performed for different frequencies by means of Eqs. (4, 5, 10). The result is shown in Fig. 2, giving BV versus the sunspot diameter $D = 2R$. We assumed a simple sunspot model with $C_S = 4.6$ km/s and $C_A = 4.9$ km/s ($B = 2000$ G) which is valid in the line-forming region of a detailed sunspot model (Staude 1981; Obridko & Staude 1988); outside $C_{Se} = 10$ km/s, and the external field is assumed to be zero. This simple model takes into account the effect of the surrounding plasma but ignores the atmospheric stratification; nevertheless it provides satisfactory agreement with the basic features of the observations, which show 'global' magnetic oscillations only in small sunspots with diameters of a few thousand km and an absence of global magnetic oscillations in large sunspots with diameters of $\gtrsim 10\,000$ km. Thus, the model of the slow body mode provides a clear explanation of the appearance of magnetic oscillations in small sunspots.

The observed value of the ratio BV in Eq. (10) sometimes exceeds two times the theoretical value. This could result from the assumption of standing waves. In this case the ratio BV is defined by (11). It could also be the consequence of our simple model that does not take into account some details such as the gradient of the magnetic field due to the divergence of the sunspot with height. Fig. 3 shows the radial dependence of slow body mode oscillations, which is defined by (6, 7), for different sunspot diameters. The values of BV strongly depends on the choice of β, which can drop up to a factor of two within the layer of optical line formation. Moreover, BV defines the amplitudes of the oscillations at a fixed optical depth. In the case of a diverging flux tube a fluctuation of the Zeeman splitting could also arise from changes of the optical depth due to perturbations of temperature and density produced by the oscillations.

The choice of the parameters outside the flux tube is not crucial for the conclusion that the magnetic oscillations are large within thin tubes. In fact, the slow body mode exists while $\delta > 1$ and the external Alfvén velocity $C_{Ae} < \omega/k$, which in the case of the slow body mode can be rewritten as $C_{Ae} < C_T$. Both conditions are always valid for sunspots, because temperature and density outside the sunspot at equal geometrical level are much higher than inside the sunspot. This is due to the Wilson depression of about 400 km between umbra and its surrounding, which exceeds several times the pressure scale height.

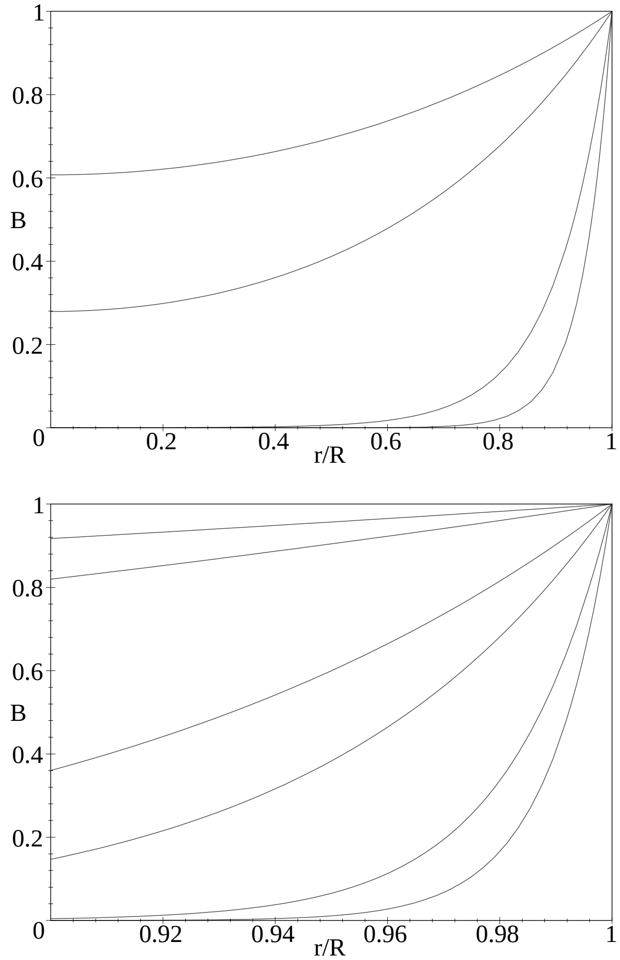

Fig. 4. Top: the dependence of the amplitude of longitudinal magnetic field oscillations B_z, normalized to its maximum value, on the radius r for the slow surface mode in units of the sunspot radius R for $R = 5$ (top curve), $50, 500$, and 1000 km (bottom curve); the period is 300 s. Bottom picture: the same with an extended r/R scale and additional curves for $R = 3000$ and 5000 km.

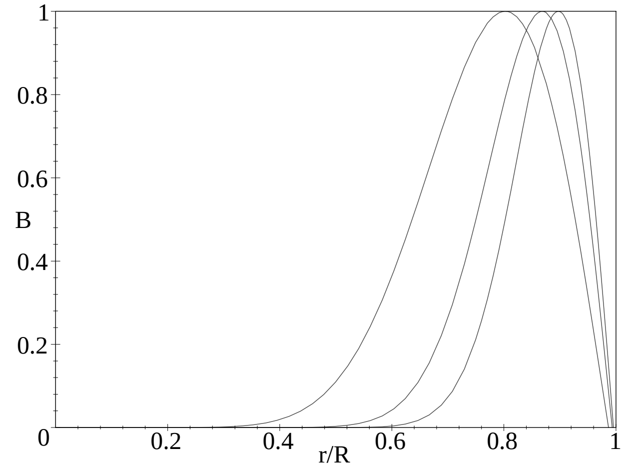

Fig. 5. The dependence of the radial part of the whispering mode, that is the radial part of the eigen-function $J_m(jr/R)$ of the longitudinal magnetic field oscillations B_z, normalized to its maximum value, on the radius r for the whispering mode, for different azimuth numbers of $m = 10$ (left curve), 20, and 30 (right curve), for a period of 300 s and $R = 5 \cdot 10^3$ km.

3.4. Magnetic oscillations in rings and arcs

A second problem is the observed non-uniform distribution of the magnetic oscillations across the umbra of large sunspots, while the velocity oscillations cover much greater parts of a spot. Obviously this hints at the coexistence of different modes of oscillations within a sunspot. Global velocity oscillations can be produced by the global slow body mode ($m = 0$), while magnetic oscillations, which are localized along the border of an umbra, could result from another wave mode which co-exists with the global mode.

3.4.1. The slow surface mode

A first natural candidate for the explanation of the appearance of the magnetic oscillations along the border is the slow surface mode. Calculations of the radial profiles of longitudinal magnetic oscillation for the surface mode are presented in Fig. 4. They suggest a minor influence on the observed structures: the surface slow mode appears as a very narrow strip (about 100 km wide) along the umbral border, which is below the resolution power of available observations. In the case of large sunspots the slow mode will appear as a narrow strip (about 40 – 50 km wide) along the umbral border of a sunspot with a radius of $R = 1000 - 5000$ km, which is far beyond the resolution of current observations. Moreover, this narrow ring would not split into details, which also contradicts the observations. The plot shows that the so-called thin flux tube approximation, which is assumed for calculating the surface mode, is valid in the solar atmosphere only for very thin flux tubes with $R < 5$ km, because the approximation supposes that the amplitude of the velocity oscillations is constant across the diameter of the tube. Of course, we cannot rule out the presence of the slow surface mode among other modes close to the umbral boundary, but we should now explore how important these other modes are for the understanding of the observed features.

3.4.2. The whispering mode

Now we focus our attention on another slow body mode with $m \neq 0$. The numerical solutions of the dispersion relation in a tube with a fixed diameter have shown that the phase speed ω/k_z of this mode tends to the tube speed C_T, when $m \to \infty$. This means that BV is defined by (10) in this limit. Thus, a slow body mode with $m \gg 1$ is an additional candidate for the explanation of magnetic oscillations. With increasing m the oscillations are concentrated in a thin arc near the boundary of the flux tube, which is shown in Fig. 5, where the dependence of the eigen-function on the azimuth ϕ has been dropped in Eqs. (6, 7).

The difference between the slow surface wave for $m = 0$, which is also concentrated at the border, and the slow body mode with $m \gg 1$ is due to the factor $\exp{(im\phi)}$, which describes a

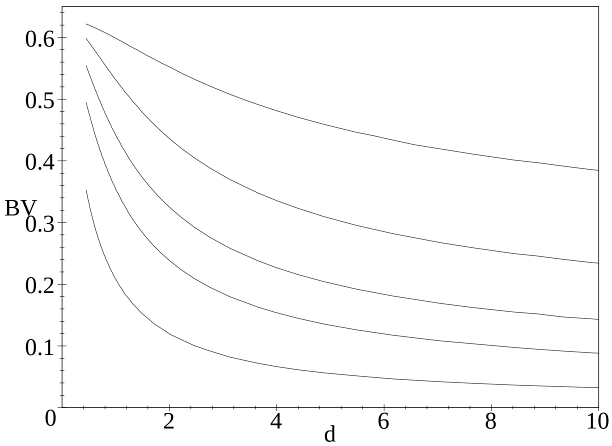

Fig. 6. The dependence of BV (see Fig. (2) for the whispering mode on the thickness of a curved strip occupied by the mode d(in 10^3 km) $= \pi R/m$, where a curvature radius of the umbral boundary of $R = 5 \cdot 10^3$ km has been chosen, for periods of 10, 5, 3, 2, and 1 min (from above to below).

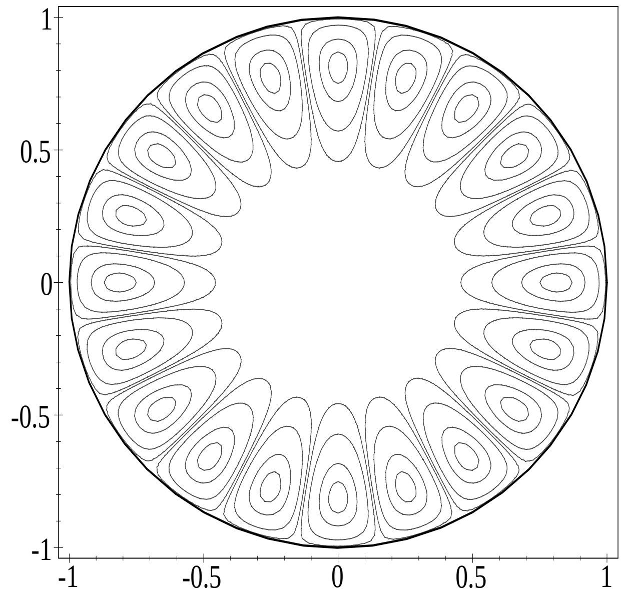

Fig. 7. The levels of equal amplitudes (0.9, 0.65, 0.25, and 0.05) of the eigen-function (6, 7) of the whispering mode, normalized to their maximum values for $t = 0$, as a function of r and ϕ for $m = 10$ and $R = 5 \cdot 10^3$ km. The oscillations in adjacent cells are in antiphase due to the factor $\cos m\phi$.

propagation of waves along the border of the tube. Fig. 7 shows the levels of equal amplitudes at a fixed moment $t = 0$ for eigen-functions normalized to its maximum value. The oscillations are concentrated along the curved border of the tube in a bunch of small-scale features.

The oscillations are almost absent in the centre of the tube, that means, their properties are governed by the curved border of the tube. The effect of concentration increases with increasing m. An approximate dispersion relation for large m is

$$\omega^2 = V_{ph}^2 \left(k_z^2 + \left(\frac{m}{R}\right)^2 \right), \tag{14}$$

where m appears as the horizontal wavenumber, and the phase velocity tends to the tube velocity $V_{ph} \to C_T$, while $m \to \infty$. In fact, m is bound for a fixed value of the frequency by the condition $k_z \geq 0$.

The mode under discussion is similar to a whispering gallery mode in acoustics, which describes the propagation of sound waves along a curved surface. It was first observed in the gallery under the dome of the cathedral of St. Peter in Rome and was explained by Rayleigh (see, e.g., Brekhovskikh & Beyer 1980). This mode also exists for electromagnetic waves; it is widely used in microlaser technology. In magnetic flux tubes the whispering mode has not been discussed so far. For $m \gg 1$ Eq. (4) can also be considered as a dispersion relation for waves propagating along a curved boundary of constant radius between the magnetized and non-magnetized plasmas. It means that it can be applied to the case when only some part of the boundary of a non-circular tube has a constant curvature. The only difference to the tube mode is that m can now differ from an integer. Such waves are being reflected from the points with abrupt changes of the radius of curvature. Thus, the whispering mode can be trapped between such points of abrupt changes of the curvature. The mode exists also at a boundary between regions with different magnetic fields. That means, it is possible to excite the whispering gallery eigen-modes at some pieces of the boundary of an umbra. The width of the strip along the boundary, where the mode is concentrated, decreases with increasing m. The vertical phase velocity of the mode tends to the tube speed, when $m \to \infty$, and the ratio of the relative amplitudes of magnetic and velocity oscillations tends to a value $\beta/\sqrt{\beta + 1}$, when the radius of the tube is fixed and $m \to \infty$. Fig. 6 shows a plot of this ratio (10) for the whispering mode, calculated for a curvature radius of the umbral boundary of $R = 5000$ km and for different frequencies as a function of the width of the curved strip occupied by the mode.

Thus, the whispering mode is a good candidate for an explanation of the concentration of magnetic oscillations along the umbral boundary.

4. The effect of stratification

Emphasis of the present paper is on the effect of the lateral boundaries of sunspots which can support modes running along arcs of constant radius. So far all treatments of sunspot oscillations considered the trapping of oscillations in sunspots due to the effect of vertical stratification. In this case the slow body waves are reflected from the upper layers due to the drop of temperature. This is valid for the widely explored mode with $m = 0$ as well as for modes with any $m \neq 0$. Thus, the whispering mode with $m \gg 1$ is subjected to reflection from the upper solar atmosphere due to the minimum of temperature between photosphere and chromosphere and to the jump of temperature at the chromosphere-corona transition region. The refraction at the bottom layers makes it possible to trap oscillations in the magnetized and in the non-magnetized solar atmosphere. In the case of the whispering mode an approximate condition of refraction $\omega^2 \approx C_T^2 m^2/R^2$ follows from the approximate dispersion equation (14). It has been mentioned before that m/R is nothing but a horizontal wavenumber.

The spectrum of the whispering mode is defined by the model of the atmosphere and the length of the arc. The value of m is defined by the condition

$$\frac{\pi}{m\Delta\theta} = 1, 2, 3 \ldots, \tag{15}$$

where $\Delta\theta$ is the length of the arc in radians. The eigen-frequency for each m is defined by the structure of the sunspot atmosphere. The eigen-frequencies are affected by the model of the surrounding atmosphere as well, if a nonzero boundary condition at the border of the tube is used. For each value of m there can exist several eigen-frequencies. This is similar to the p-modes, which have many eigen-frequencies for every l value. Thus, an m value corresponds to an l value for a sunspot. The number of eigen-frequencies and their values for fixed m are defined by the structure of the subphotospheric layers of the sunspot and the shape of the subphotospheric flux tube. Thus, it is not suprising that the observations (e.g. those of Balthasar 1999) reveal multi-frequency magnetic oscillations along the border of a large sunspot.

Fig. 1 shows that the magnetic oscillations along the umbral border of the large sunspot form two almost closed circles side by side. The two circles can be interpreted as two separate whispering modes, which appear due to the special shape of the sunspot, the umbra of which looks like a bundle of two flux tubes. The smooth run of the curvature appears interrupted, changing its sign at two opposite points on the umbra-penumbra border. A reflection of the whispering mode from these points should be produced, but this is not observed. This is why we speculate that the two tubes forming the sunspot are separated below the photosphere, thus making it possible to produce two circles of magnetic oscillations.

5. On some alternative interpretations

It has been suggested to us that an alternative to the interpretation in terms of an $m \gg 1$ eigenmode would be random, localized excitations near the umbra-penumbra boundary. However, the problem of an excitation of sunspot oscillations cannot be treated without considering eigen-mode oscillations, because excitation means excitation of wave modes, which do exist in the physical object under consideration. For example, the distribution of the energy across a laser is completely defined by the properties of the resonator. The same holds for the distribution of the energy of oscillations over a sunspot. Of course, if the excitation is localized near the umbral boundary, the excitation of the whispering mode has to dominate over the excitation of modes with low m. The mechanisms of excitation and damping of oscillations define which modes (with which m) exist in sunspots. Such a discussion of sunspot oscillations is not the topic of the present paper.

The current observations show a concentration of the energy of magnetic oscillations along the sunspot umbral border. Slow body modes with $m \gg 1$ are a good candidate for an explanation. At first sight the filamentary structure of the magnetic field near the umbral boundary could be an alternative candidate for the interpretation. This would correspond to Parker's spaghetti model. In fact, the distances between the tubes are smaller than the wavelengths of the oscillations and they cannot oscillate independently. The ensemble of flux tubes has to support collective modes of oscillations, which are similar to the slow mode oscillations with $m = 1, \gg 1$, and to all intermediate modes. Of course, the spaghetti structure of the boundary of a sunspot can impose some restrictions on the choice of possible m. On the other hand, the spaghetti model can provide an explanation of the fine structure of the distribution of energy of oscillations across large sunspots, such as it is visible in Fig. 8 of the paper by Balthasar (1999).

6. Discussion

The first emphasis of our paper is on the possibility of sunspot eigen-modes with $m \neq 0$, while $m = 0$ has been considered so far in all publications. The new observations with high spatial resolution clearly show the fine structure of the oscillations. Their distribution can be considered as an effect of the fine structure of the subphotospheric magnetic field of the sunspot (spaghetti model). But this should not be considered as an alternative explanation. Just the multi-mode approach is relevant for the spaghetti model, because the spatial separation of tubes is not large enough to treat their oscillations as independent from each other.

The second emphasis is on the slow body wave model of sunspot oscillations providing an explanation of two types of magnetic field oscillations: those concentrated in small sunspots due to the mode with $m = 0$ as well as those in rings and arcs along the umbral boundaries in larger sunspots due to the whispering gallery mode with $m \gg 1$. The possibility to explain the magnetic oscillations in both cases is an advantage of the multi-mode approach. Shortcomings of our model, such as the neglect of the atmospheric stratification and of the divergence of the sunspot with height, do not affect the basic capability of slow body waves to produce strong magnetic oscillations only on small scales. An advantage of the treatment of a stratified model with uniform magnetic field is the possibility to to find out the eigen-frequencies. In principle it is necessary to combine both approaches. However, this is a difficult problem, which has not been solved so far, because in this case the problem cannot be reduced to the consideration of ordinary differential equations.

The observed values of the relative magnetic oscillations – Eq. (10) – are almost two times larger than the theoretical predictions. However, both the theoretical and the observational results have to be regarded with caution, because the accuracy of present observations is still low, and the theoretical model does not take into account the gradient of the magnetic field and of other quantities with depth. The last is a shortcoming of all models published so far.

The measurement of phase differences between Doppler shifts and magnetic oscillations is an effective tool to explore the sunspot oscillations. The observations of Horn et al. (1997) provide the phase shift between oscillations of the longitudinal magnetic field and velocity. These results could be explained by standing slow body waves, which have a node for the velocity at the level of the photospheric observations. The phases of the oscillations of longitudinal magnetic field and velocity coincide in this case for the slow body waves, because their phase velocity $V_{ph} = \omega/k_z$ is in the range $C_T < V_{ph} < C_S$, and the factor $\omega^2 - k_z^2 C_S^2 > 0$ is positive in Eqs. (6–7). However, this agreement has to be considered with caution, because the model does not take into account a magnetic field gradient with depth and replaces the consideration of evanescent waves by standing waves, which is not always correct. In the observations of Balthasar (1999) the magnetic oscillations are governed not only by the longitudinal magnetic field, but by a combination of δB_r and δB_z, thus making the interpretation of observations rather complicated.

The discovery of the magnetic field oscillations shows that a modelling of sunspot oscillations as a single-mode oscillation is inadequate. The occurrence of the whispering mode in sunspots is highly probable because it explains not only the localization of magnetic oscillations along the umbral border, but also very easily their trapping in sunspots. Even a small difference in the temperatures inside and outside the sunspot, which will exist in deeper subphotospheric layers too, can provide the trapping.

In small sunspots and pores the whispering mode could exist in addition to the 'global' slow body mode with $m = 0$. However, such an extremely narrow arc could hardly be discovered in the presently available data. There are examples of small features with observations of velocity oscillations without magnetic oscillations. They can be explained by the fast mode which does not produce large magnetic oscillations on small scales.

The main result of our present study is that sunspot oscillations cannot be understood as a one-mode oscillation only. In large sunspots the slow body waves with $m = 1, 2, 3 \ldots$ can be resolved by a cross correlation analysis of Doppler shifts across the spot and distinguished from the whispering modes with $m \gg 1$ due to the absence of magnetic oscillations. In small sunspots the slow body modes with $m > 0$ also produce a pattern of oscillations, which are 180^o out of phase in the different parts of the umbra. These modes cannot be resolved by the available resolution; in the small spots the smearing of the oscillations will remove modes with $m \gg 1$ and reduce the amplitudes of modes with $m > 0$ in favor of the fundamental mode with $m = 0$. This effect is similar to the observation of p-modes of the Sun as a star. Eigen-oscillations with $m = 0$ appear at a few frequencies, exactly as in the case of p-modes with $l = 0$; this can be seen in the spectra of magnetic oscillations in small sunspots (Fig. 5 by Balthasar 1999). The oscillations are not only multi-mode oscillations, but multi-frequency oscillations as well. It cannot be ruled out that for the first time the signature of the fine structure of the spectrum of sunspot oscillations has been observed in our data.

Magnetic oscillations in small dark patches, which are located within the penumbra, are visible in our observations as well (see Fig. 1). The white-light picture of Fig. 1 shows, that the patches are really small umbrae imbedded in the penumbra. Thus, measurable magnetic oscillations in these patches support our general conclusion, that magnetic field fluctuations appear only on small scales, which are created by a small scale of the magnetic field along with a small scale of the wave mode itself due to $m \gg 1$. So far, the restrictions of the model and of the observations do not permit to compare observations and theory in more detail.

Acknowledgements. We thank an anonymous referee for critical comments and questions that made us sharpen our arguments and correct misprints. The authors gratefully acknowledge financial support of the present work by the German Science Foundation (DFG) under grant Nos. 436 RUS 113/81/2 and /4. The VTT is operated by the Kiepenheuer-Institut für Sonnenphysik, Freiburg, at the Spanish Observatorio del Teide of the Instituto de Astrofísica de Canarias.

References

Balthasar H., 1998, In: Rimmele T.R., Balasubramanian K.S., Radick R.R. (eds.) High Resolution Solar Physics. Proc. 19th NSO/SacPeak Summer Workshop. ASP Conf. Ser. 183, p. 100
Balthasar H., 1999, Solar Phys. 187, 389
Bendlin C., Volkmer R., Kneer F., 1992, A&A 257, 817
Brekhovskikh L.M., Beyer R.T., 1980, Waves in Layered Media. 2nd Edition, Applied Mathematics and Mechanics 16, Academic Press, New York – London, p. 419
Edwin P.M., Roberts B., 1983, Solar Phys. 88, 179
Gore A., 1998, Solar Phys. 178, 13
Gurman J.B., Leibacher J.W., 1984, ApJ 283, 859
Horn T., Hofmann A., Balthasar H., 1996, Solar Phys. 164, 321
Horn T., Staude J., Landgraf V., 1997, Solar Phys. 172, 69
Lites B.W., 1992, In: Thomas J.H., Weiss N.O. (eds.) Sunspots: Theory and Observations. NATO ASI Series C 375, p. 261
Lites B.W., Thomas J.H., Bogdan T.J., Cally P.S., 1998, ApJ 497, 464
Norton A.A., Ulrich R.K., Bogart R.S., Bush R.I., Hoeksema J.T., 1998, In: Deubner F.L., Christensen-Dalsgaard J., Kurtz D. (eds.) New Eyes to See inside the Sun. IAU Symp. 185, p. 453
Norton A.A., Ulrich R.K., Bush R.I., Tarbell T.D., 1999, ApJ 518, L123
Obridko V.N., Staude J., 1988, A&A 189, 232
Roberts B., 1992, In: Priest E.R., Hood A.W. (eds.) Advances in Solar Magnetohydrodynamics. Cambridge University Press, p. 105
Roberts B., Webb A.R., 1978, Solar Phys. 56, 5
Rüedi I., Solanki S.K., 1999, In: Schmieder B., Hofmann A., Staude J. (eds.) Magnetic Fields and Oscillations. 3rd Advances in Solar Physics Euroconference, ASP Conf. Ser. 184, p. 131
Rüedi I., Solanki S.K., Stenflo J.O., Tarbell T.D., Scherrer P.H., 1998, A&A 335, L97
Scheuer M.A., Thomas J.H., 1981, Solar Phys. 71, 21
Staude J., 1981, A&A 100, 284
Staude J., 1999, In: Schmieder B., Hofmann A., Staude J. (eds.) Magnetic Fields and Oscillations. 3rd Advances in Solar Physics Euroconference, ASP Conf. Ser. 184, p. 113
Thomas J.H., Scheuer M.A., 1982, Solar Phys. 79, 19
Uchida Y., Sakurai T., 1975, PASP 27, 259
Wood W.P., 1997, Solar Phys. 173, 259
Žugžda Y.D., Locāns V., Staude J., 1983, Solar Phys. 82, 369
Žugžda Y.D., Staude J., Locāns V., 1984, Solar Phys. 91, 219
Žugžda Y.D., Locāns V., Staude J., 1987, Astron. Nachr. 308, 257